Identification of Karstic Features in Lateritic Soil by an Integrated Geophysical Approach

P. Anbazhagan, Divyesh Rohit, Athul Prabhakaran & B. Vidyaranya

Pure and Applied Geophysics
pageoph

ISSN 0033-4553
Volume 175
Number 12

Pure Appl. Geophys. (2018)
175:4515-4536
DOI 10.1007/s00024-018-1908-8

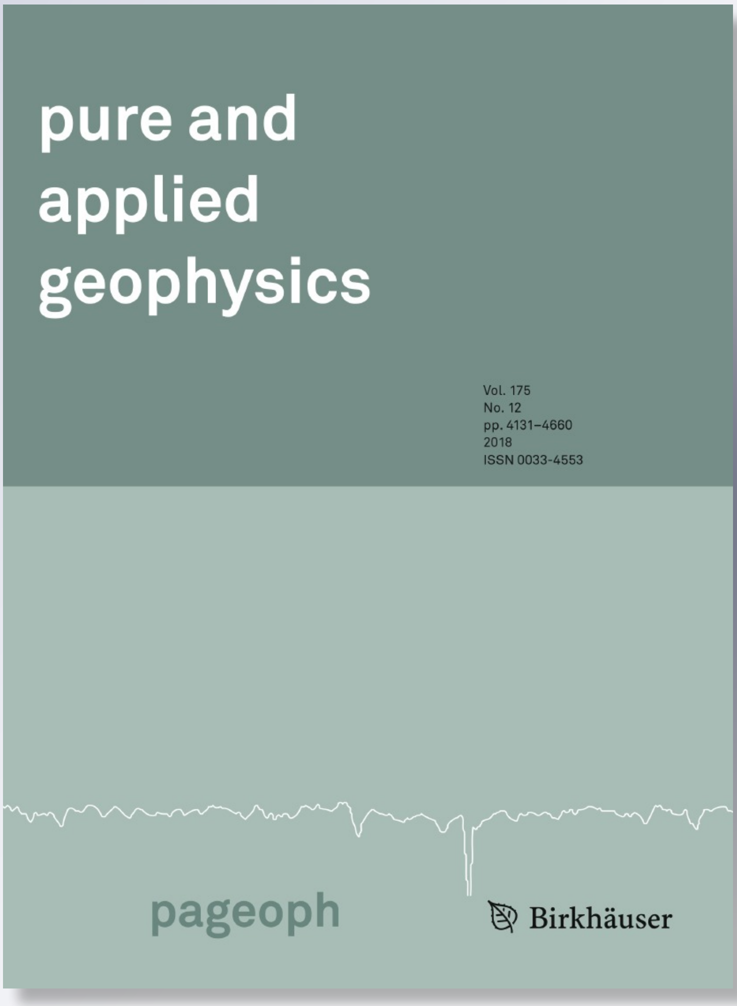

Pure Appl. Geophys. 175 (2018), 4515–4536
© 2018 Springer International Publishing AG, part of Springer Nature
https://doi.org/10.1007/s00024-018-1908-8

Pure and Applied Geophysics

Identification of Karstic Features in Lateritic Soil by an Integrated Geophysical Approach

P. Anbazhagan,[1] Divyesh Rohit,[1] Athul Prabhakaran,[1] and B. Vidyaranya[2]

Abstract—Lateritic soils are widely spread across the southern and central parts of India. Lateritic formations usually have soft sediments, entrapped between hard to medium soft lateritic rock, which are leached due to the ingress of water during rainy seasons creating hollow sections or cavities which span over large lengths. Laterites are highly heterogeneous and prone to cavitation due to its weathering process; a sound knowledge of the subsurface condition is required before starting any construction. This study presents the application of integrated geophysical investigation for the identification of cavities at a mega construction site in Kerala State, India. Geophysical survey methods, namely ground penetrating radar (GPR) and multichannel analysis of surface waves (MASWs) techniques, are used to identify the heterogeneities in lateritic soils and localized cavities. The survey areas identified are critical sections of a mega construction project subjected to heavy dynamic and static loads. The preliminary GPR survey is carried out across the study areas at specific interval spacing to identify probable heterogeneities. Confirmative survey or detailed GPR and MASW surveys are carried out at the locations identified in the preliminary survey at close intervals to confirm the presence of an anomaly and identify its location. The anomalies in the GPR radargram are identified by visual inspection and trace amplitude approach. Using MASW survey, a 2D shear wave velocity profile is generated to identify low shear wave velocity zones which confirm the presence of an anomaly. On comparing the data from both GPR and MASW survey techniques, the underground cavities were successfully identified at multiple locations with further crosschecking with borings. The study further provided details on subsurface lithology at survey locations.

Key words: GPR, MASW, laterite soil, cavities, integrated geophysical techniques.

1. Introduction

The word 'Laterite' was originally coined in India by Francis Buchanan, a Scottish physician referring to a type of residual soil resulting from tropical weathering under conditions of high rainfall, intense leaching, and oxidation (Gidigasu 1976). The lateritic soils of the Malabar region are characterized as a weak rock which is typically used in making bricks for low-to-medium rise buildings and non-load bearing walls (Kasthurba et al. 2007). Lateritic soils are known for heterogeneity and karstic features like sinkholes, underground cavities and soil piping (Anirudhan 2014). Such problems were identified and documented through a geophysical investigation in Kannur District, Kerala (WTS Limited 2013).

Multiple reasons have been attributed to the formation of cavities and sinkholes in the lateritic soil in the literature. Based on the study of sinkholes in peridotite rock mass in Australia, it was found that similar behavior in laterites was mainly due to two reasons, firstly due to the removal of silica and silicate minerals by solution which percolate deeper in the joints formed by underlying limestone, and secondly due to the collapse of ferricrete cap into voids (Twidale 1987). Typical laterite lithology in the Western Ghats has mottled zone consisting of a red honeycomb-like structure with voids filled with yellowish or pinkish to white kaolinite clay overlying a crust layer. The honeycombing framework becomes lighter and the size of the cavities or voids increases with depth. The materials in the voids are type of soft clay which on exposure to continuous cycle of wetness and dryness and could be washed away (Bhagyalekshmi et al. 2015). The soil piping in southern regions of Western Ghats is caused due to the influence of a combination of physical, chemical, hydrological and tectonic factors. The factors contributing to soil piping are rainfall exceeding 5 cm/h threshold limit, a high concentration of sodium, low concentrations of calcium and magnesium, sandy texture at shallow depths, vicinity to lineaments in

---

[1] Department of Civil Engineering, Indian Institute of Science, Bengaluru 560012, India. E-mail: anbazhagan@iisc.ac.in; anbazhagan2005@gmail.com

[2] L&T EDRC, Mumbai, India.

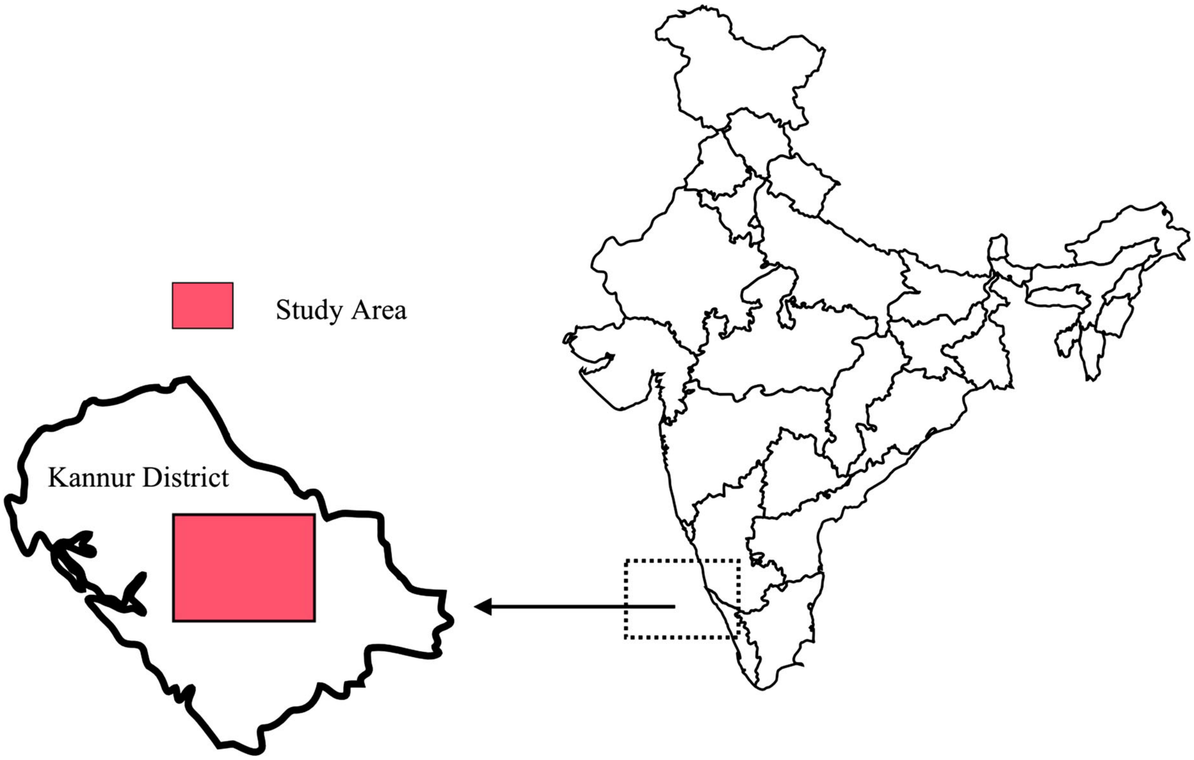

Figure 1
Location of study area in Kannur District, Kerala, India (map not to scale)

regions of tectonic stress development and deforestation (Bhagyalekshmi et al. 2015). Identification and location of sinkholes in Malabar region are of major interest for researchers and engineers as large sinkholes serve as zones of preferential recharge to aquifers. These sinkholes might collapse at any time and catastrophic in nature for the built environment if not identified at an early stage. Karstic features like soil piping can pose a significant impact on the effective hydraulic conductivity and storm run-off generation in slopes, which could lead to slope failures (Uchida and Mizuyama 2002).

The unpredictable collapse of soil pipe roofs concealed beneath the earth became a high disaster in the highland regions of Idukki District, which lies in the Malabar region. This phenomenon has destroyed cultivable lands and man-made structures, destabilized the topography and modified the subsurface hydrology (Bhagyalekshmi et al. 2015). A subsurface investigation using boreholes and samples collection is inefficient and ineffective in providing the subsurface profile and spatial variation of soil lithology. Conventional methods are inefficient, time-consuming and provide limited data at specific points, which need to be interpolated spatially to obtain a complete subsurface profile. The Range of geophysical techniques can be used effectively to detect the presence of caves and voids below the surface over large areas (Cardarelli et al. 2010; Gambetta et al. 2011; Kaufmann et al. 2011; Andrej and Uroš 2012). Microgravity methods which identify local cavities on the basis of density contrast between the cavity and host rock are widely used to identify cavities in limestone (Samsudin 2003). Individual geophysical methods are known to have deficiencies and hence an integrated approach by multiple methods is proposed using a two-tier framework to isolate subsurface anomalies (Anbazhagan 2015). The successful applications of each individual method depend on factors including geological conditions, target type, size and location of the target (Orfanos and Apostolopoulos 2012).

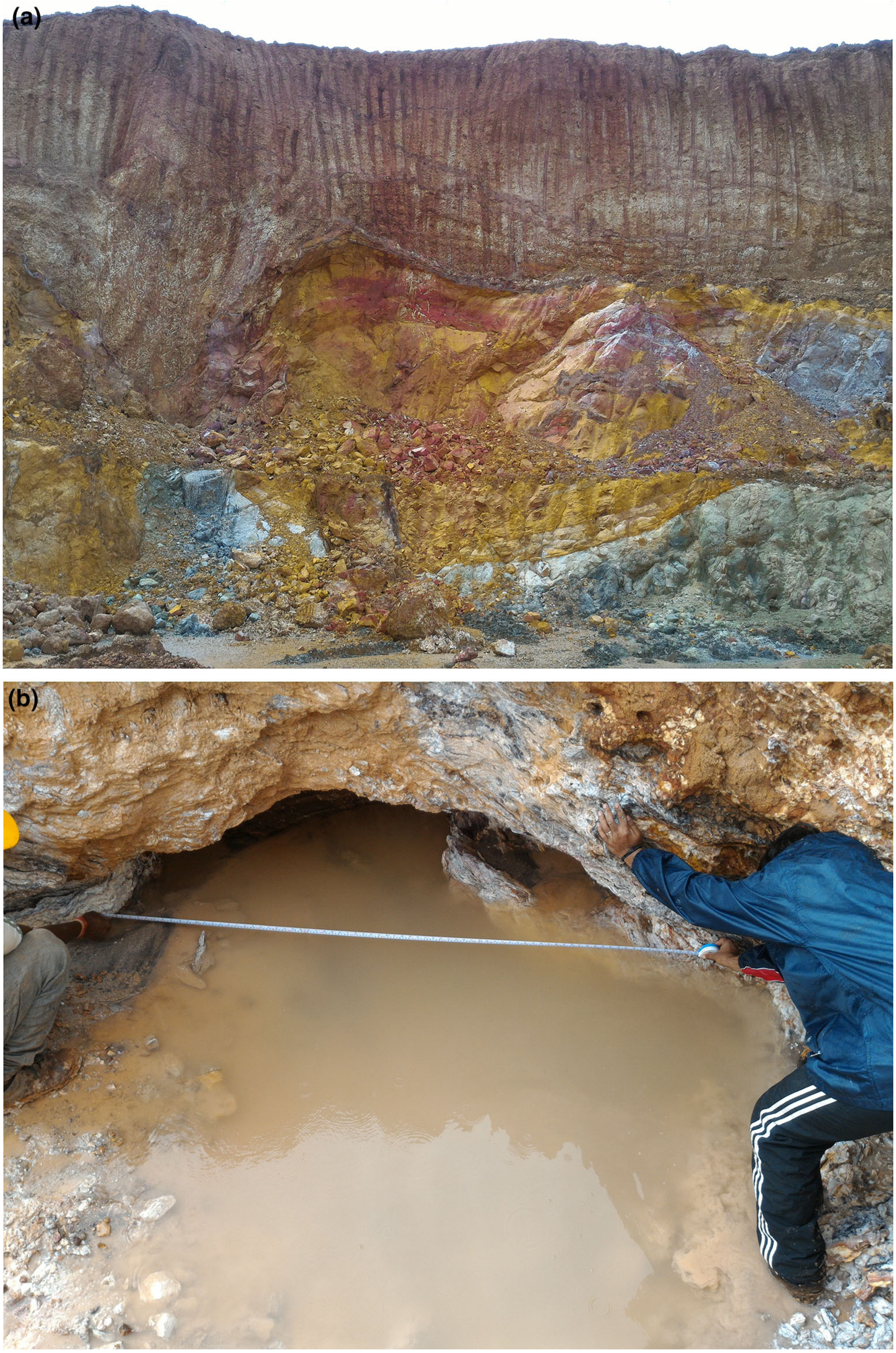

Figure 2
a Soil stratification across a vertically cut wall and **b** cavity with water flow

Geophysical methods like ground penetrating radar (GPR) and seismic refraction are widely used in the subsurface identification of heterogeneities, sinkholes in karst and lateritic terrains in past decades. The identification of karstic features with geophysical methods is mainly based on a geophysical contrast between the anomaly and the surrounding rock (El-Qady et al. 2005). The applicability of GPR survey is feasible and effective in smooth terrain for shallow depths (few meters), with no or less moisture and fine grained soil (Reynolds 1997) and so this survey has been used in this study as an initial screen to study the subsurface profile. The radargram is checked for any anomalies which are then isolated for detailed survey. In lateritic deposits, seismic refraction technique (e.g., multichannel analysis of surface wave, MASW) was used in addition to point testing methods for identification of a location as well as spatial details like the 2D-subsurface profile of cavities (Anirudhan 2014). The combined information from radargram and the 2D shear wave velocity profile provides sufficient details to obtain an idea on nature of the identified anomaly at the site.

Identification of cavities caused by sinkholes by integrated use of seismic refraction tomography, MASW, GPR and electrical resistivity tomography data is given by Dobecki and Upchurch (2006). Though lateritic soils are wide spread in Western Ghats of India and frequent cases of cavity collapse are reported, very limited scientific studies are presented to identify cavities well in advance and treat the same to minimize damages. The present study aims at identifying and locating these subsurface karstic features using integrated geophysical approach, to facilitate adequate improvement measures in advance to mitigate failure due to collapses of hidden/underlain cavities. Further, the subsurface layers will be interpreted based on the relative dielectric contrast.

Figure 3
Survey using 100 MHz GPR antenna over known cavity location

Figure 4
Data acquisition using MASW survey by placing geophones at 1 m spacing

2. *Study Area*

The study area under investigation is approximately 400,000 m^2 of a large-scale project located in Malabar region of Kerala, India. Figure 1 shows the study area. GPR survey over entire study area was carried out in grid lines of 2.5 m intervals in first screening, and closer interval of 1.5 m grids during resurvey. The site has a humid tropical climate with mean daily temperature ranging from 16 to 35 °C. The precipitation of region is influenced by two monsoons, the southwest monsoon from June to September and northeast monsoon from October to December. As the site lies on the windward side of Western Ghats, the major amount of rainfall occurs during the southwest monsoon. The average annual rainfall is 3438 mm. While 70% of rainfall occurs during June to September, the northeast monsoon contributes only 30% rainfall.

The geological formations of the region are of Archaean to recent age (Narayanaswamy 2004). Archaean formation mainly consists of gneisses and charnockites. The study was conducted in Kannur Coastal Region, which geologically is recent bed coastal alluvium. Also, residual laterite of sub-recent age occurs as a thick blanket over the crystalline and sedimentary formation and forms the major lithology of the area (Prasad 2014). Though Kerala has both high and low level laterites, those found in the study area are low level laterites and detritus in nature. They are of secondary origin which are derived from high-level laterites and recombined after deposition in the valleys or plains (Wadia 1945). Kerala experiences slope stability problems, slump, creep, subsidence (Anbazhagan and Sajinkumar 2011; Sajinkumar et al. 2011). The laterites of the region are highly heterogeneous and stratified in nature with high susceptibility of underground cavity formation (Fig. 2a, b).

3. *Methodology*

As the study area is very large, it was uneconomical and ineffective to adopt point exploration methods in a highly variable stratum like laterite. Hence, initially a GPR survey was carried out and locations containing GPR anomalies were identified by rapid visual interpretation of the radargrams to be further investigated by both GPR and MASW. The identified area was surveyed in a grid pattern by GPR to isolate the anomaly to be further surveyed

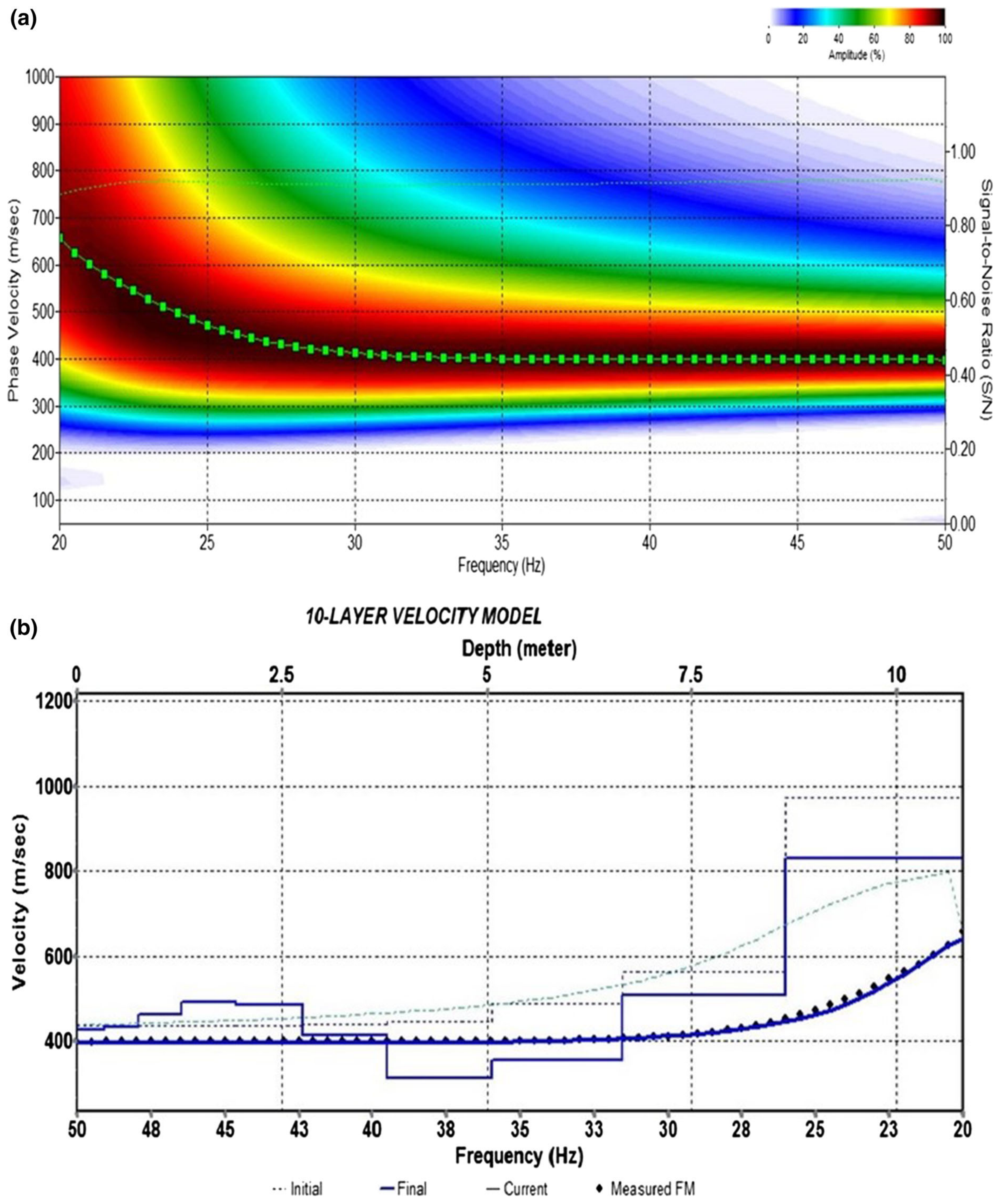

Figure 5

a Typical dispersion curve of MASW survey over lateritic soil and **b** typical 1D shear wave velocity profile

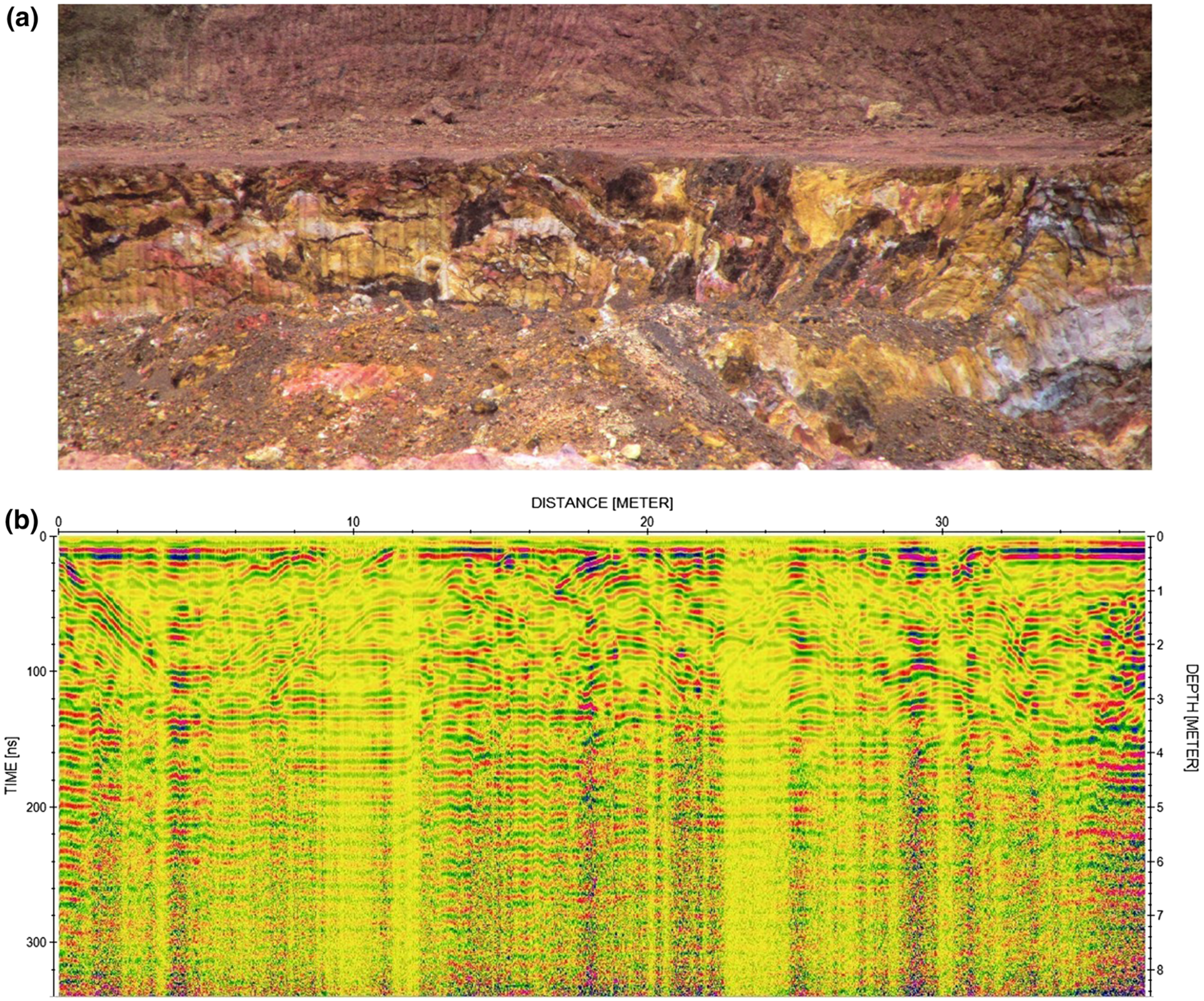

Figure 6

a Face of a typical cut-section with lithological undulations and **b** radargram showing the lithological undulations in the cut-section

using MASW. The detailed MASW survey was conducted to provide dimension to the findings of the GPR survey in identifying the nature of the heterogeneity. The survey was limited to excavated regions as the uncertainties below ground shall be high due to the removal of overburden. In locations with an average height of filling close to 5 m, heterogeneities below that level may not be interesting to engineering as stresses are minimized within the subgrade level. GPR survey is carried out in these areas. Geophysical methods like GPR and MASW adopted for study are briefed in the subsections below.

3.1. GPR Survey

In the present study, Mala ProEx 100 MHz (Fig. 3) and 500 MHz continuous waves, ground coupled, shielded bi-static antenna GPR system are used for the investigation. The maximum penetration depth of Mala ProEx 100 and 500 MHz antennas is around 15 and 5 m, which depend on the ground conditions like soil type, moisture content, salt content, etc. The preliminary survey was conducted over the identified areas of the construction site by 100 MHz frequency antenna longitudinally along the length at regular intervals of 2.5 m apart. The distance traversed by GPR equipment was measured

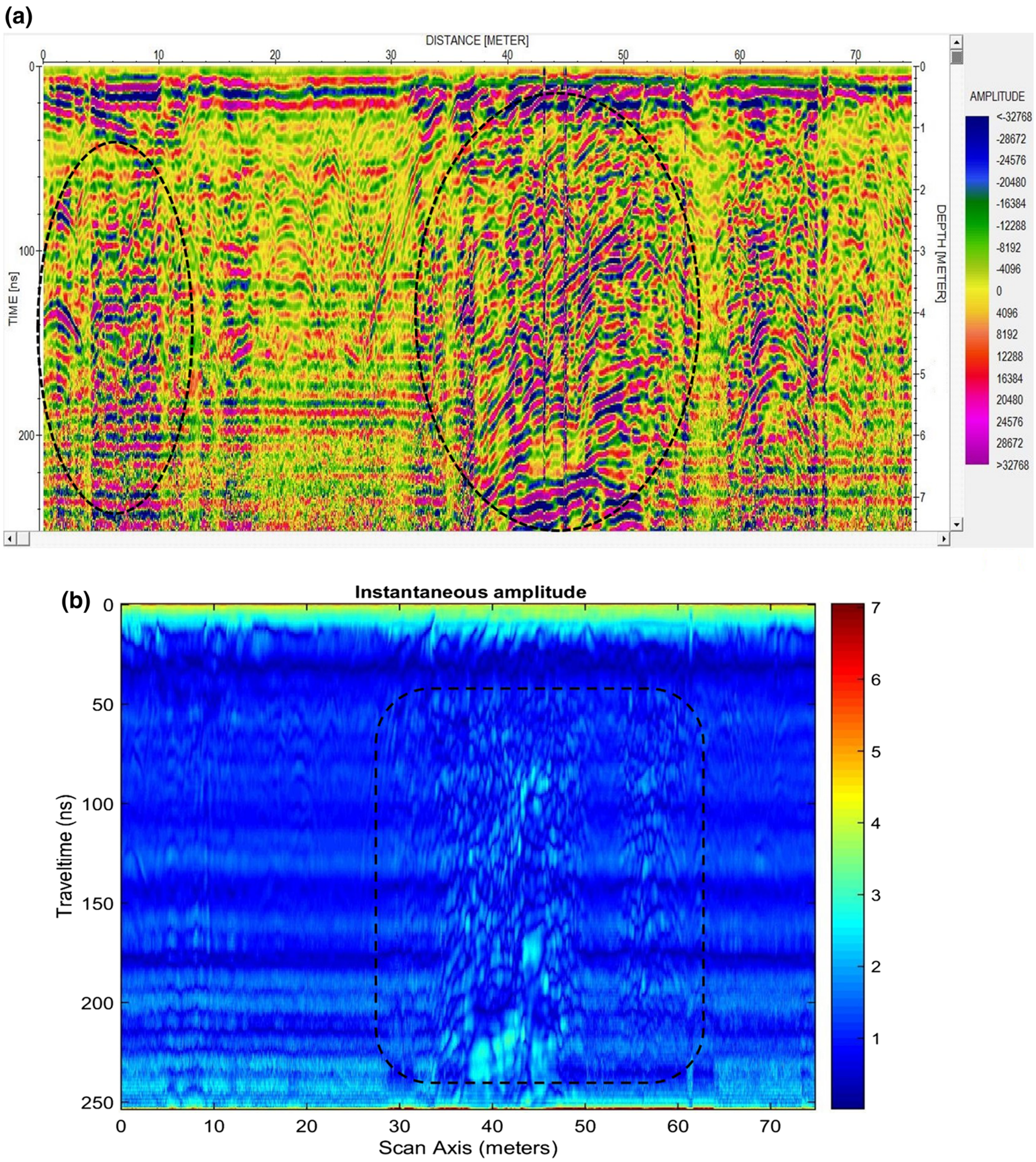

Figure 7

a Processed radargram for 100 MHz antenna, **b** instantaneous amplitude of the radargram over the heterogeneous region with higher signal amplitude as seen in the region enclosed with the dashed line and **c** 2D shear wave velocity map for the survey over heterogeneous region showing no significant contrast in the shear wave velocity

by standard distance measuring wheel attached to an antenna. 500 MHz antenna is used for the confirmative survey to obtain high-resolution 2D images of the subsurface. The processing of raw GPR data performed with RadExplorer (Deco Geophysical 2008) and REFLEXW Software (Sandmeier 2009) by

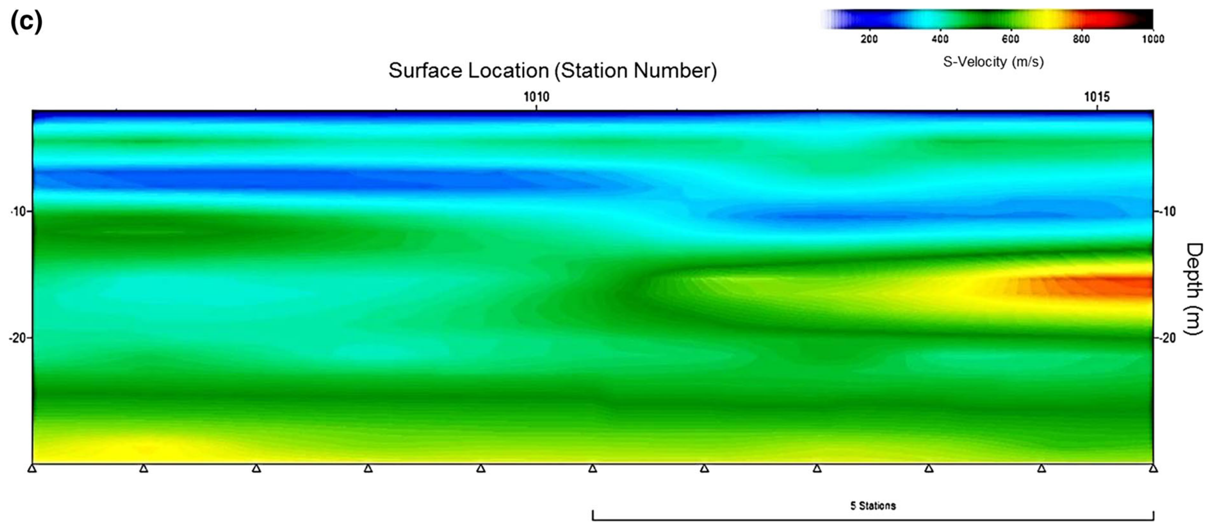

Figure 7
continued

applying: static correction to adjust the vertical position of the surface reflection; DC removal which removes the arithmetic mean component from each trace of the radargram individually. Band-pass Butterworth filter with four frequency values to reduces noise with distinct frequency content and linear gain, to emphasize the low amplitude ranges against high amplitude ones. After processing, instantaneous amplitude was obtained using MATGPR 3.0 (Tzanis 2006) software. Hilbert-transformation (linear operator and quadrature filter) is used to determine the instantaneous amplitude of the data which gives an evaluation of the reflectivity and is analogous to the square root of signals total energy at a given instant of time (Claerbout 1985). In radargrams, the instantaneous amplitude is a measure of the reflectivity strength (Tzanis 2006). For the current study, a uniform wave velocity of 0.08 m/ns is used resulting in relative permittivity of 3.5.

3.2. Seismic Survey

The seismic survey helps in determining the geotechnical properties of a subsurface material by means of measuring surface wave dispersion. The surface wave survey method is the most convenient way to determine the elastic properties of the shallow subsurface material. Sinkholes filled with loose gouge have lower shear wave velocity than the surrounding material; hence, this contrasting velocities can help in identification of sink holes. In the existing literature, Ferland (1969) documented using a modified seismic refraction array to locate and map air-filled voids with collapsible features in dolomite and limestone. MASW emphasizes on the dispersion of Rayleigh type surface waves (Park et al. 1999). As a large portion of the Rayleigh wave is shear, hence, the lateral variation in V_s are imaged using MASW. Similar to GPR, in MASW higher frequency geophones provide higher resolution data at shallower depths and low frequency geophones provide data till deeper depths (Nolan et al. 2013). The usage of MASW is cost-effective and time-efficient, using one dataset we can apply three different studies (i.e., 2D shear velocity section, amplitude mapping, and P wave seismic refraction), which can be combined for cavity detection (Almalki and Munir 2013). The MASW survey was performed using 12 or 24 channel seismograph with 4.5 Hz geophones (Fig. 4). The seismic wave for this survey is generated from an active source (a 7 kg sledgehammer on a 300 mm × 300 mm × 25.4 mm size metal plate). Figure 5a, b shows typical dispersion curve of lateritic soil and the shear wave velocity.

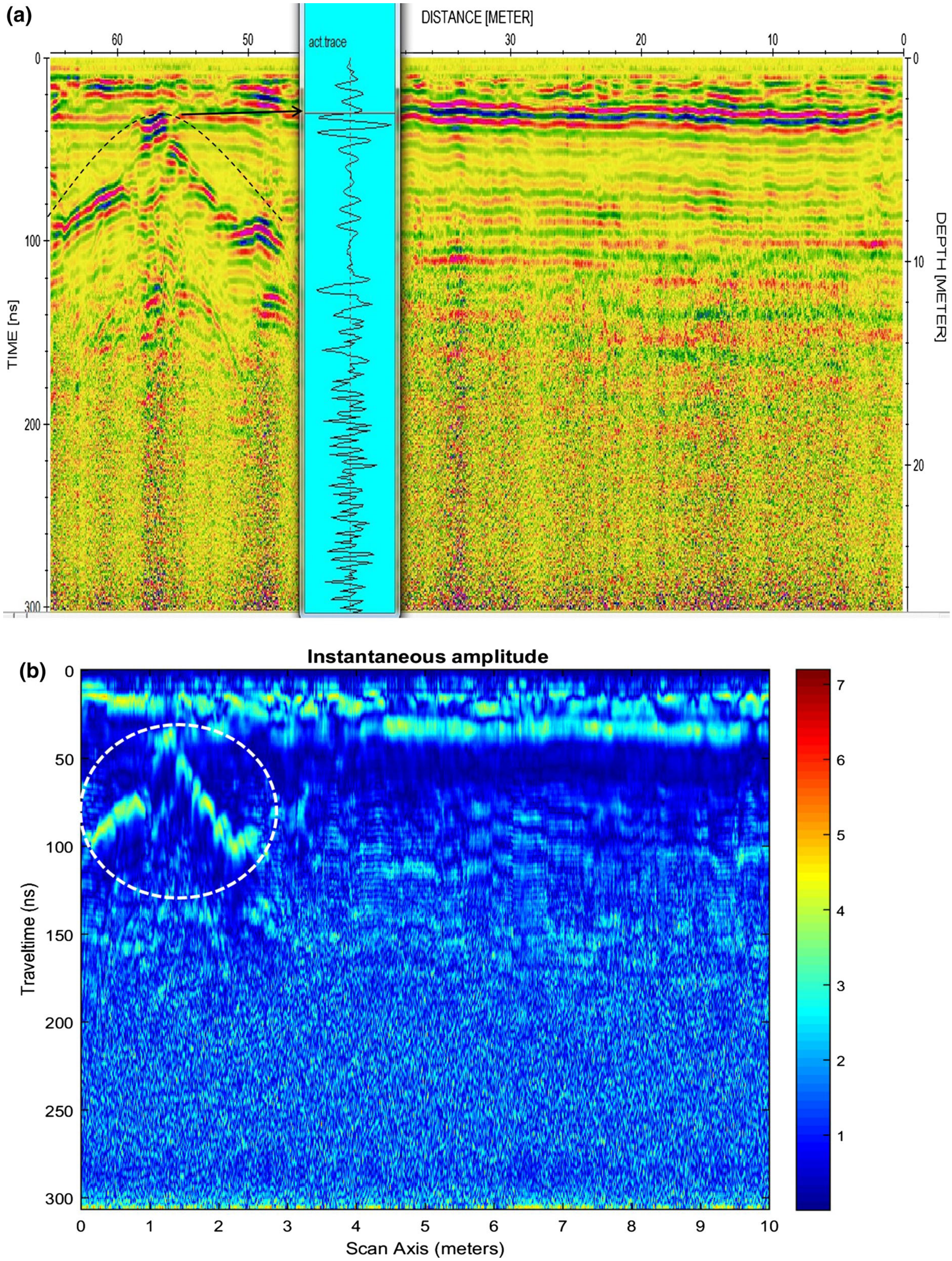
(a)
DISTANCE [METER]
60
50
30
20
10
0
act.trace
TIME [ns]
0
100
200
300
DEPTH [METER]
0
10
20
(b)
Instantaneous amplitude
Traveltime (ns)
0
50
100
150
200
250
300
Scan Axis (meters)
0
1
2
3
4
5
6
7
8
9
10
1
2
3
4
5
6
7

◀Figure 8
a Processed radargram for 100 MHz antenna, **b** instantaneous amplitude of the radargram, **c** 2D shear wave velocity map and **d** borehole data representing underground cavity. The hyperbolic signature is highlighted by a dashed curve and the black arrow indicates the peak in signal amplitude at the elevation of cavity

4. *Results and Discussion*

An understanding of the difference between karstic and non-karstic signatures is paramount in interpreting results; hence, cavities with surface feature manifestations are used to study the GPR signal. The subsections illustrate the mapping of a surface cavity feature at two Locations 1 and 2 with 500 and 100 MHz antennae, respectively, and their confirmation with MASW survey. Further two typical cases of unknown karstic locations have been discussed with detailed discussion of results from radargrams as well as 2D shear wave velocity images.

4.1. *Differentiating Between Karstic Reflection and Non-karstic Reflection*

Using only one geophysical method like GPR to identify karstic features in highly heterogeneous media may not provide confirmative results as GPR radargrams are interpreted through dielectric contrasts and, hence, the exact nature of the anomaly is not fully realized. It was observed that such contrasts could be attributed to a variety of reasons including the presence of boulders in soil and curved layer formations due to soil deposition process. This section depicts how geophysical signatures from karstic features can be differentiated from other non-karstic features using integrated geophysical techniques. Figure 6a, b shows the respective face profile and radargram of a typical location. It can be noticed that a number of hyperbolic signatures may be interpreted as a cavity due to low data quality. A cut at location shows that hyperbolic signatures even correlate well with soil layering, which could lead to a false interpretation. Initial studies confirmed that conventional ways of radargram interpretation, i.e., hyperbolic signatures may not be the best suitable way to interpret voids. Systematically scanned GPR radargrams have been created and anomalous identified or doubtful locations are screened for further study. 2D MASW surveys are carried out at specified locations to generate a subsurface shear wave 2D velocity profile. Figure 7a–c shows the radargram image, instantaneous amplitude of the radargram signal and 2D shear wave velocity profile, respectively, at an anomalous subsurface location identified using GPR. Here, though an anomaly can be observed in the radargrams (Fig. 7a, b), the 2D shear wave velocity profile confirms the presence of heterogeneities in the area (Fig. 7c).

To understand the unique character of the karstic features, GPR and MASW surveys are carried out on top of a previously identified cavity location. The 2D radargram for 100 MHz GPR antenna over an actual/known cavity shown in Fig. 8a and the instantaneous trace amplitude is seen in Fig. 8b. The corresponding shear wave velocity profile over the cavity can be seen in Fig. 8c which confirms the presence of voids validating the credibility of integrated survey techniques. The peak observed in GPR trace amplitude in radargram is caused due to dielectric contrast caused between air cavity and the surrounding earth material (Fig. 8a). In GPR radargrams, the peak amplitude signal trace is shown as solid line arrow and hyperbolic signature is highlighted by a dashed curve. The radar signal amplitude is changed at the reflecting boundary depending on the dielectric contrast and the thickness of the layer (Fig. 8b). Also, a velocity contrast zone can be observed in the shear wave velocity profile conducted over air cavity (Fig. 8c). MASW survey results technically confirm the existence of loose gouge in the localized zone. Further, the 2D shear wave velocity profile is also useful to interpret deeper layers and contrast zones, providing additional insight. The results of both GPR and MASW surveys are justified by boreholes (Fig. 8d) drilled at the respective survey locations. Here, cavities are identified at around 3 m from the surface in each of the three boreholes BH-1–3.

4.2. *Mapping of Cavity Alignment*

In the site, after heavy rain, it was noticed that continuous water was gushing out on surface at Location 1. Here, a cavity with the surface feature is identified after water was found flowing through the

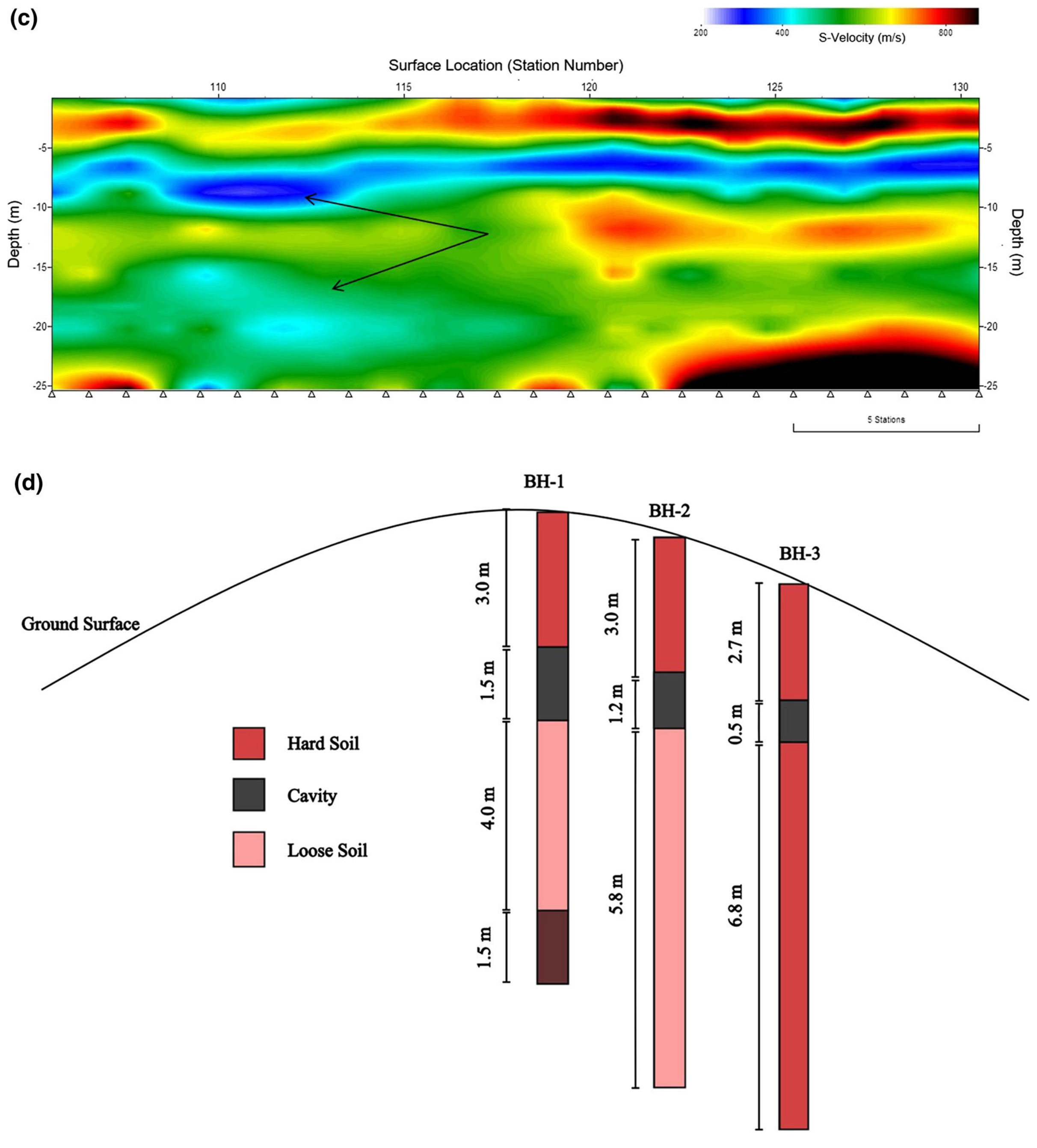

Figure 8
continued

fissure created by construction activity as seen in Fig. 9. The opening in the ground surface is an irregular shape with a very hard lateritic layer on the surface; the fissure and flow of water are visible by clearing top soil. It is observed that the top surface of the cavity is hard enough to carry the load of a passenger car. GPR and MASW surveys are carried out at this location to verify the karstic signatures as discussed in the previous sections. Due to its shallow nature, a higher frequency antenna of 500 MHz is

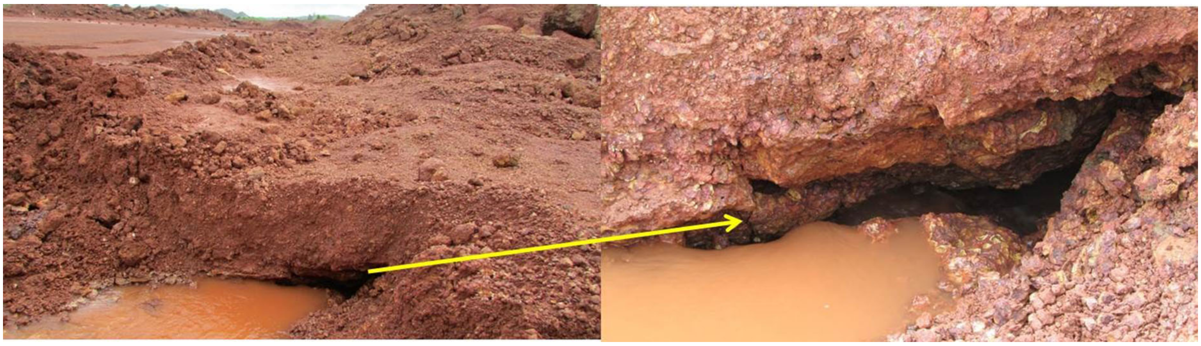

Figure 9
Water gushing through the cavity

used for exploration. The processed radargram image for 500 MHz antenna (Fig. 10a) with instantaneous amplitude (Fig. 10b) and 2D shear wave velocity profile of subsurface are shown in Fig. 10c. In Fig. 10a, the dielectric contrast at the soil–air interface confirms the presence of a cavity. Figure 10b depicts the instantaneous amplitude of the radar signal which is a representation of the signal strength. Further, in Fig. 10c the karst could be identified through a low velocity region in the shear wave velocity profile. The high velocity region present at the bottom could be a probable boulder or rock.

4.3. *Size and Depth of Cavity*

A small circular subsidence is observed due to an air cavity below the surface (Fig. 11) at Location 2. As seen from Fig. 11 the internal structure seems to be eroded due to washing of fine sand from the pores under constant variation of the water table. Similar to Location 1, as discussed above, the surrounding surface layer was hard enough to carry heavy loads without highlighting the presence of a soil pipe below. GPR and MASW surveys are carried out to map size and depth of the cavity. The processed radargram image for 100 MHz antenna (Fig. 12a) with instantaneous amplitude (Fig. 12b) and 2D shear wave velocity profile (Fig. 13) of subsurface are provided. Here, two parallel MASW surveys are conducted 2 m apart for a better view of the shape and extent of the cavity which could not be ascertained through a visual inspection from the surface. The results of both the surveys are in agreement with each other and with GPR radargram outputs. Integrated approach not only helps to identify karst but also size and depth of karst feature below the surface. These data are useful to decide the level of treatment required to close cavities by economical design.

4.4. *Cavity at Unknown Locations*

From the above discussion, it is very clear that combined GPR and MASW surveys help to map karstic features in problematic soils. The study area was scanned systematically using GPR and doubtful locations are identified and detailed resurveys are carried out at doubtful locations by both GPR and MASW. Cavities identified at fresh locations without any surface manifestation are discussed in the following sections.

Typical location where an anomaly was observed in the initial scanning of GPR is further investigated by integrated GPR and MASW surveys. Figure 14a depicts the processed radargram of the 100 MHz GPR antenna and Fig. 14b shows the strength envelope of the radargram highlighting the cavity. GPR radargram with hyperbolic signature and higher amplitude pulse highlights the presence of air cavities. Figure 15 shows the 2D shear wave velocity profile at the same location in longitudinal and cross-sectional orientation, respectively. The MASW surveys carried out in two directions to identify the exact location for drilling. From the radargram, the cavity can be identified by a hyperbolic signature with a

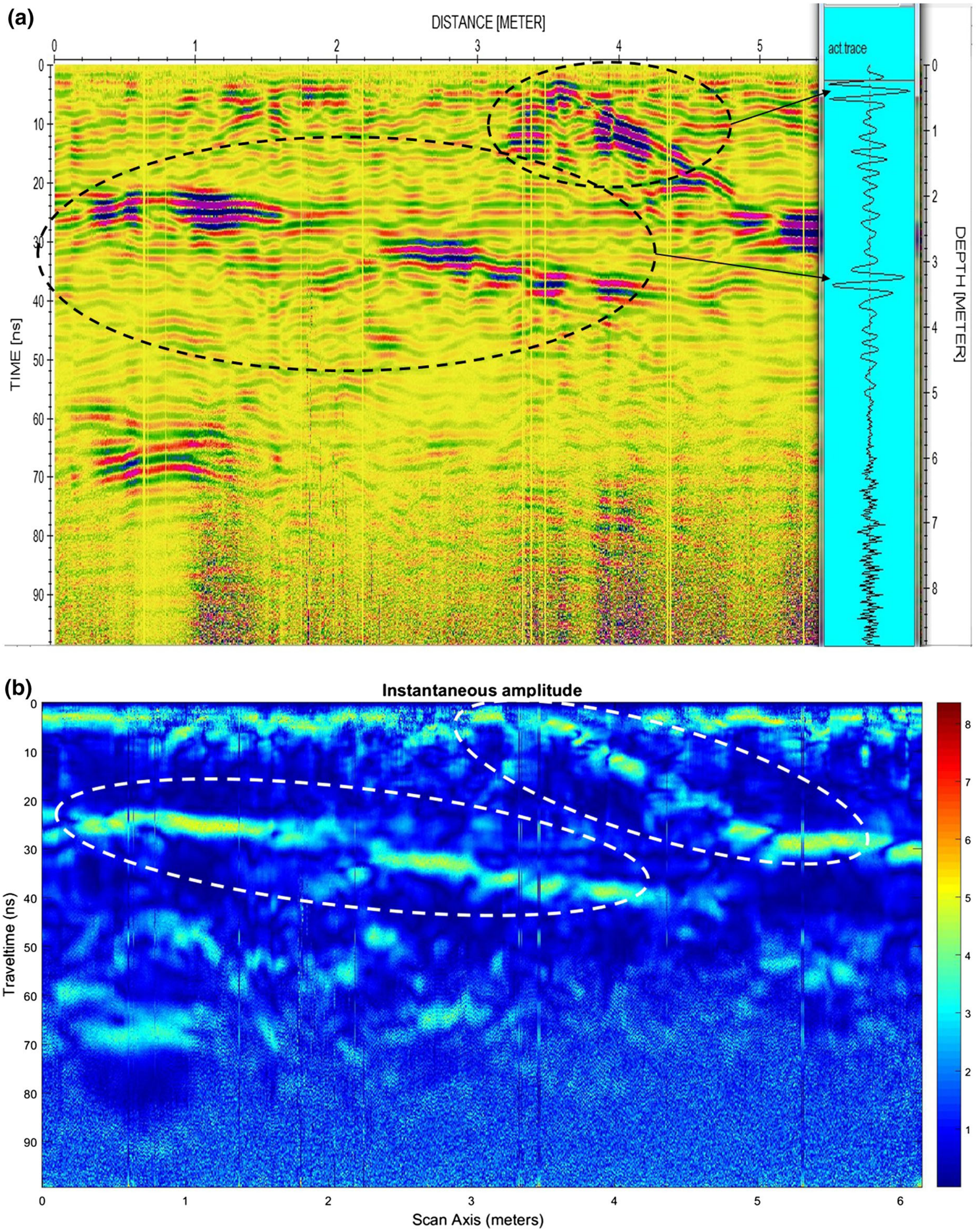

Figure 10

a Processed radargram for 500 MHz antenna over the cavity, **b** instantaneous amplitude of the radargram at Location 1 and **c** 2D shear wave velocity map. The encircled zones with higher contrast indicate the presence of cavity. The black arrows in 2D shear wave velocity profile indicate low velocity zones confirming the presence of cavity

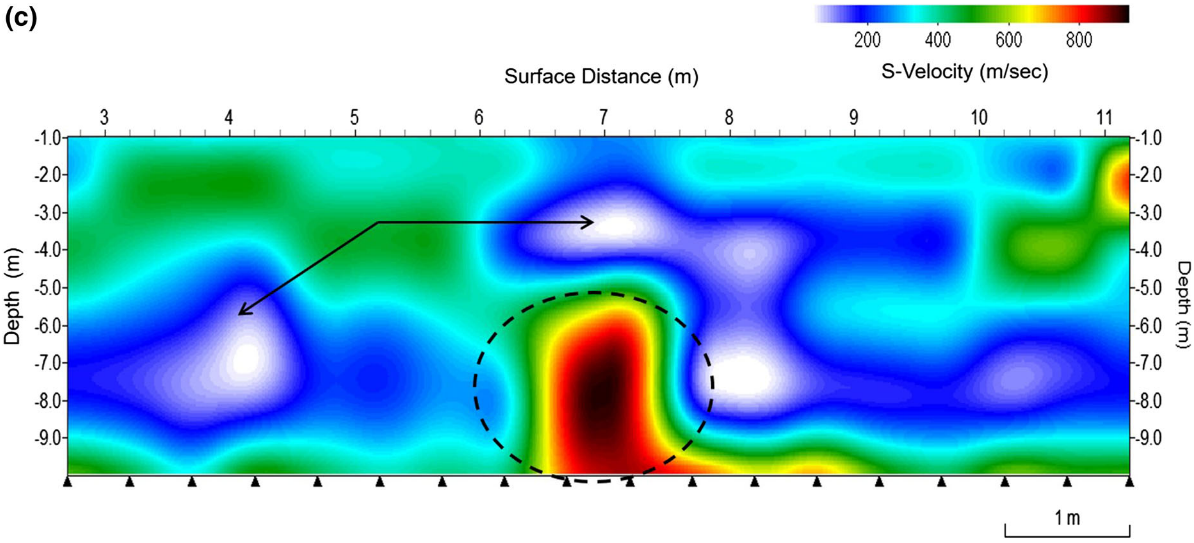

Figure 10
continued

Figure 11
Top surface of soil pipe with internal structure in chronological order at Location 2

high signal amplitude and instantaneous amplitude. It is clearly visible from the radargram that the signal shows a sudden spike in amplitude while passing through the air cavity–soil interface. Also, the 2D shear wave velocity profiles show a significantly low velocity in velocity profile for cavity than the nearby areas. The integrated survey confirmed the presence

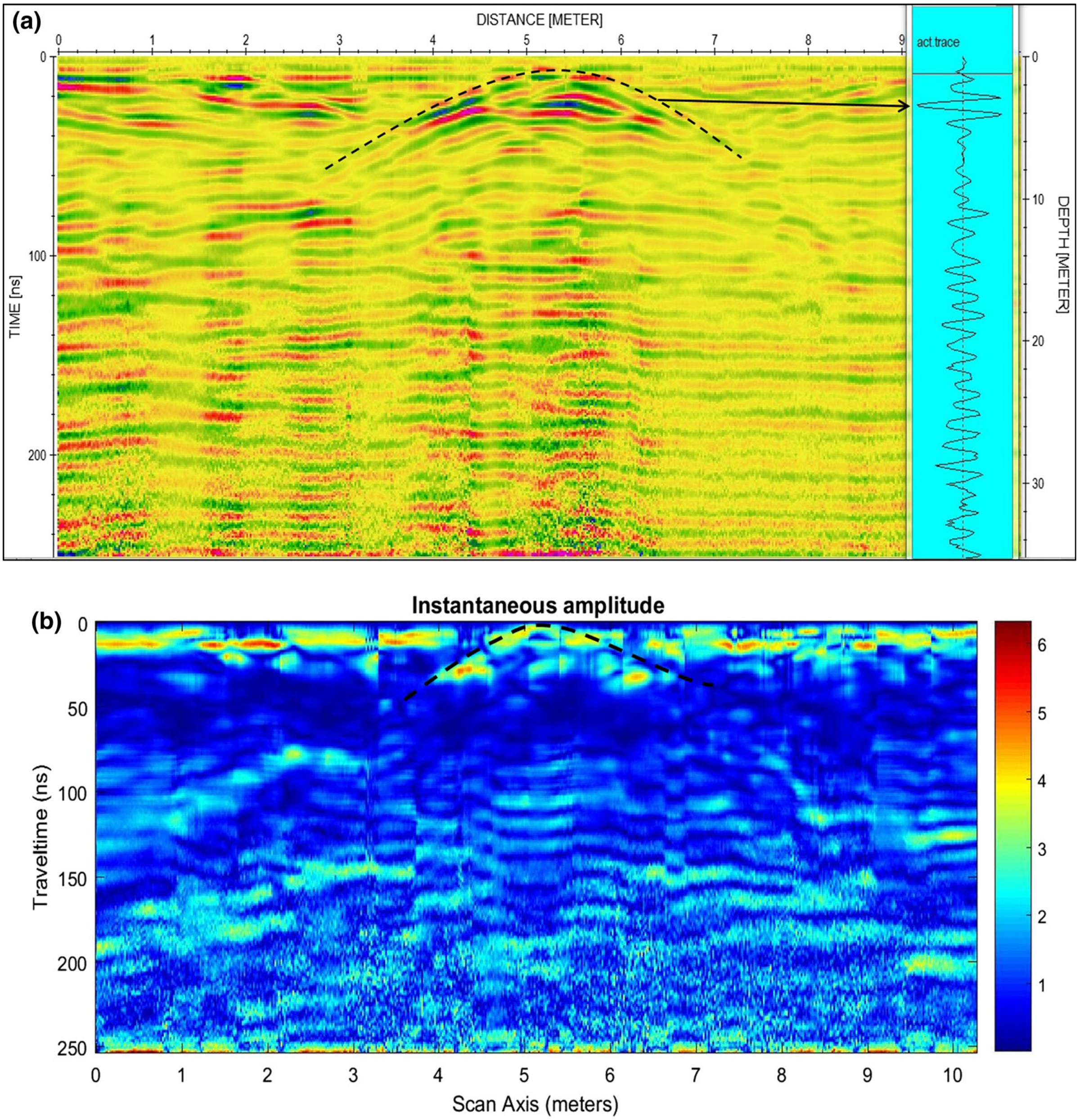

Figure 12

a Processed radargram for 100 MHz antenna over the cavity and **b** instantaneous amplitude of the radargram at Location 2. The hyperbolic signature is highlighted by a dashed curve and the black arrow indicates the peak in signal amplitude at the elevation of cavity

of the cavity at around 4 m depth which needed to be treated to avoid future collapsing.

In another typical location, the GPR survey was done just as the ground was cleared of plants and shrubs for construction purposes. A MASW survey was conducted after an interval of a few days from GPR survey during which a soil cover of around 1 m was placed over it. Figure 16a, b depicts the processed radargram and instantaneous amplitude of the 100 MHz GPR antenna and Fig. 16c represents 2D shear wave velocity profile of the same subsurface. From the radargram, the cavity is identified by a

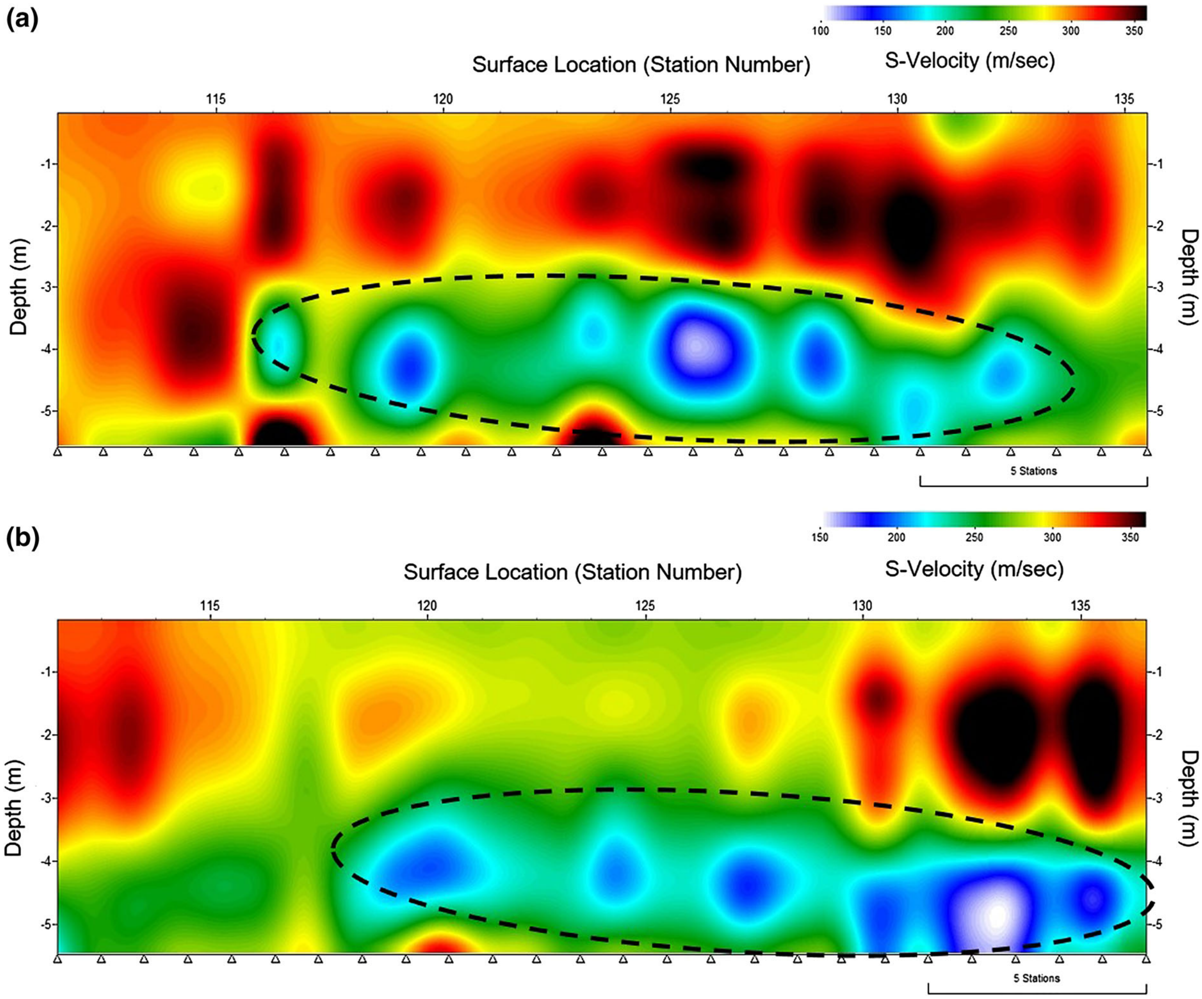

Figure 13
2D shear wave velocity map for parallel survey performed at Location 2 over the cavity. The dashed encircled region indicates low velocity zones, confirming the presence of cavity

hyperbolic signature with high instantaneous amplitude. In Fig. 16a, a sudden spike in the signal amplitude is seen when it passes through an air cavity–soil interface below the ground surface, which usually dampens with depth. Also, the 2D shear wave velocity (Fig. 16c) profile shows a significantly low velocity region in the velocity profile than the nearby earth material, which confirms the presence of non-rigid material or air cavity. The integrated survey confirmed the presence of the cavity at around 3–4 m depth. The presence of the cavity is further validated at the site by drilling boreholes to the desired depths.

5. *Conclusions*

The objective of this study is to investigate the location of karstic features like soil pipes, cavities and natural water collecting sinkholes in lateritic soils by integrated geophysical testing. From the existing literature, it is known that laterite soils have a honeycomb-like structure with small cavities. These cavities tend to increase in size and wash off under continuous variation of the water table. In this study, two geophysical methods, namely GPR and MASW, are used to perform integrated subsurface

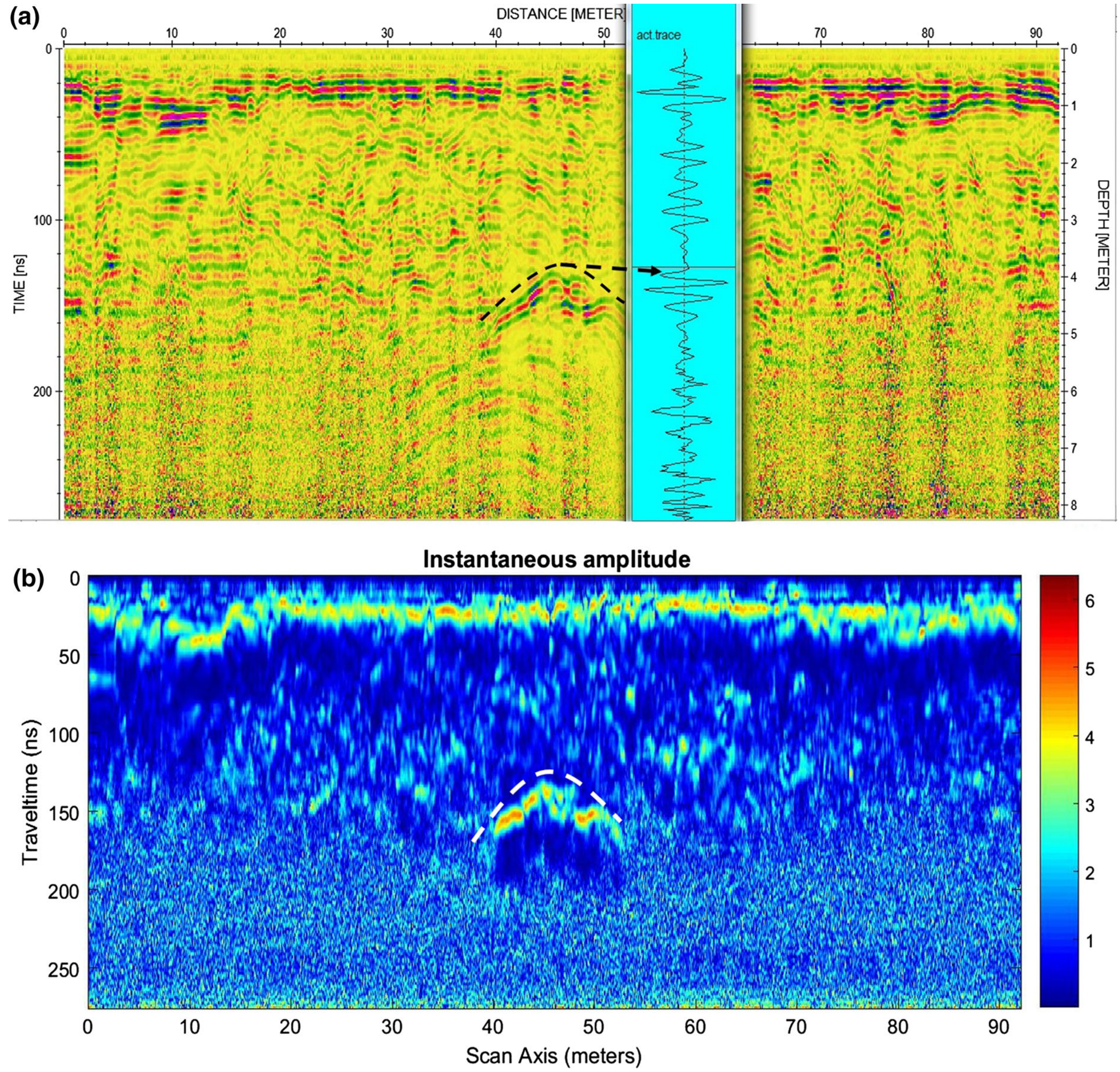

Figure 14

a Processed radargram for 100 MHz antenna over the cavity and **b** instantaneous amplitude of the radargram at Location 3. The hyperbolic signature is highlighted by a dashed curve and the black arrow indicates the peak in signal amplitude at the elevation of cavity

investigations. These methods help capture vast area of about 400,000 m^2 efficiently as compared to point methods. Preliminary GPR survey is carried out to mark anomalies; these marked areas are rescanned in finer intervals and MASW surveys are carried out to confirm the presence of a cavity.

As a sharp dielectric contrast is observed between cavity and host rock that generates readily distinguishable anomalies. In this study, the use of integrated geophysical surveys is presented as a case study to highlight the shortcomings of a single method can be overcome using integrated techniques. The difference between signals from karstic features and other heterogeneities demonstrated the need for additional dimensionality when using only GPR surveys. From the study, it was found that the use of

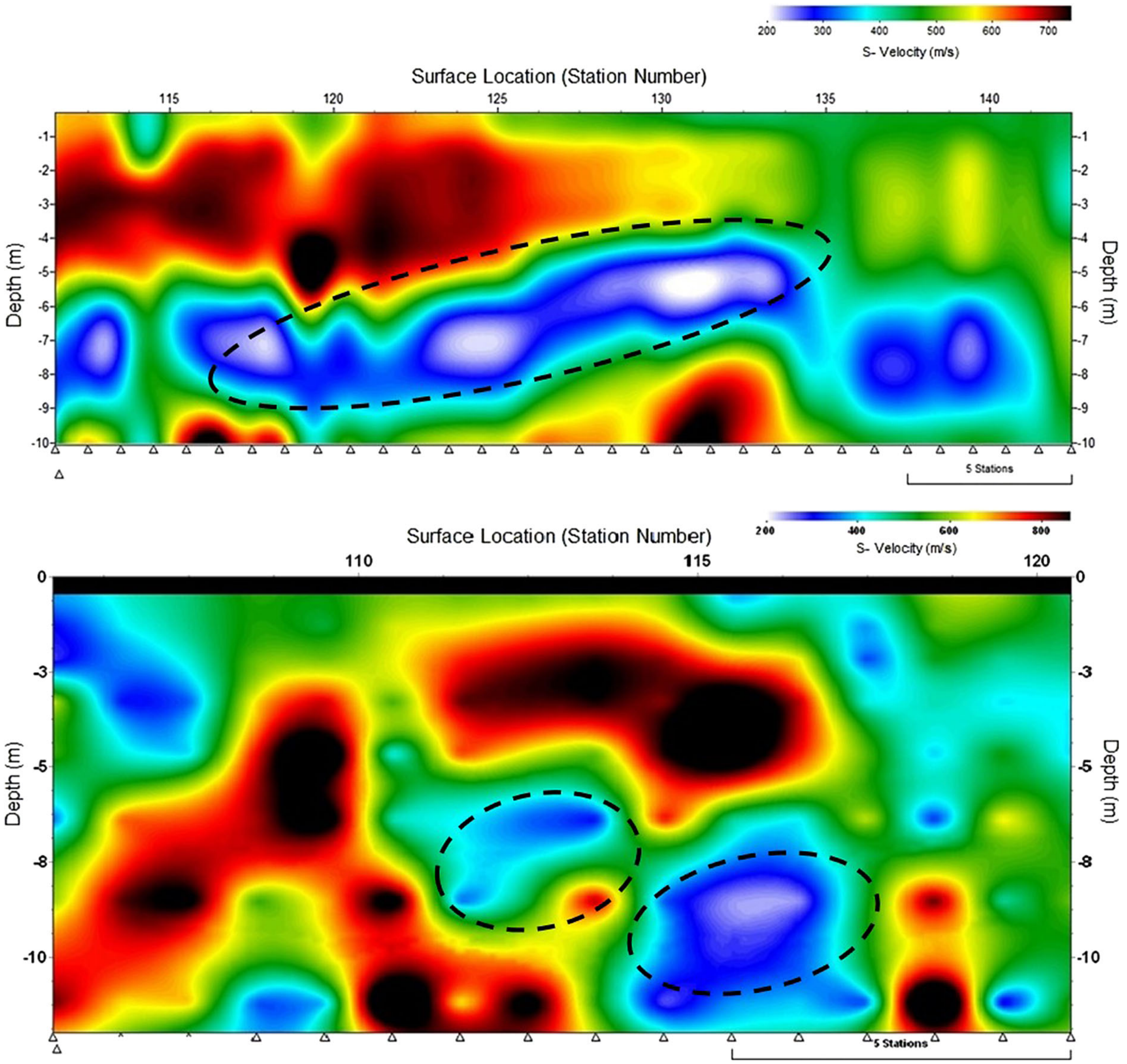

Figure 15
2D shear wave velocity map for MASW survey performed at Location 2 over the cavity, along and across the GPR survey line over unknown cavity. The dashed encircled region indicates low velocity zones, confirming the presence of cavity

higher frequency antenna for near surface or shallow investigation provided higher and better resolution. Also from the MASW survey, the presence of cavity is confirmed by low velocity zones surrounded by high velocity zones. In the case of damp or saturated soils where the ability of GPR decreases, MASW can be used effectively to identify cavities. The results obtained from the survey helped in identifying

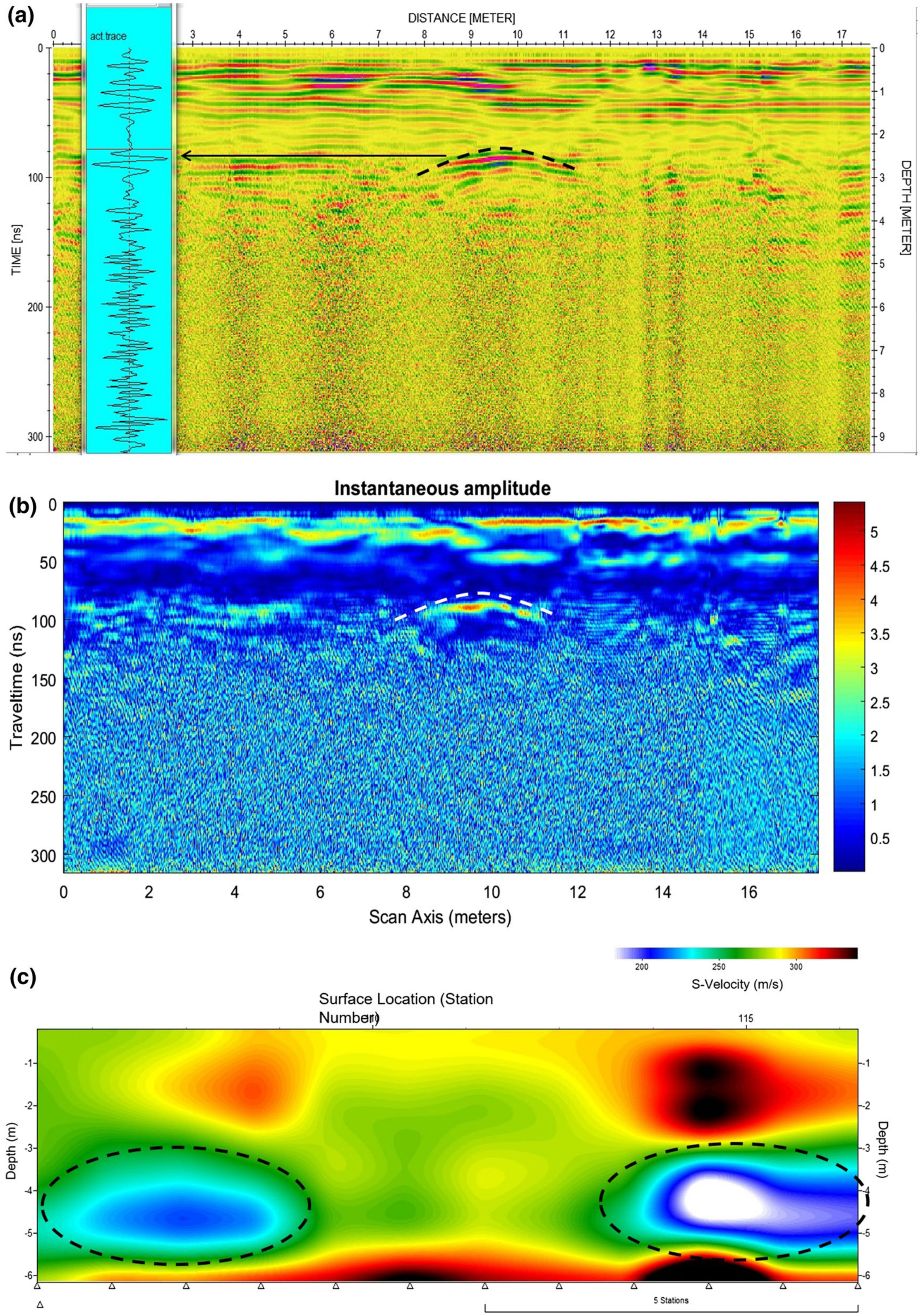
(a)
DISTANCE [METER]
0 3 4 5 6 7 8 9 10 11 12 13 14 15 16 17
act.trace
TIME [ns]
0 100 200 300
DEPTH [METER]
0 1 2 3 4 5 6 7 8 9
(b)
Instantaneous amplitude
Traveltime (ns)
0 50 100 150 200 250 300
0 2 4 6 8 10 12 14 16
Scan Axis (meters)
5 4.5 4 3.5 3 2.5 2 1.5 1 0.5
(c)
200 250 300
S-Velocity (m/s)
Surface Location (Station Number)
110
115
Depth (m)
-1 -2 -3 -4 -5 -6
5 Stations

◀Figure 16
a Processed radargram for 100 MHz antenna over the cavity, **b** instantaneous amplitude of the radargram at Location 4 over unknown cavity and **c** 2D shear wave velocity map. The hyperbolic signature is highlighted by a dashed curve and the black arrow indicates the peak in signal amplitude at the elevation of cavity. The dashed encircled region indicates low velocity zones, confirming the presence of cavity

cavities at unknown locations, which otherwise shall be hazardous due to sudden subsidence on loading.

REFERENCES

Almalki, H., & Munir, K. (2013). Efficiency of seismic attributes in detecting near-surface cavities. *Arabian Journal of Geosciences, 6,* 3119–3126.

Anbazhagan, P. (2015). Integrated subsurface investigation of the misaligned reinforced soil retaining wall. *Indian Geotechnical Journal, 45*(3), 332–340.

Anbazhagan, S., & Sajinkumar, K. S. (2011). Geoinformatics in terrain analysis and landslide susceptibility mapping in parts of Western Ghats, India. In S. Anbazhagan, S. K. Subramaniam, & X. Yang (Eds.), *Geoinformatics in applied geomorphology* (pp. 291–315). Boca Raton, FL: CRC Press.

Andrej, M., & Uroš, S. (2012). Electrical resistivity imaging of cave Divaška jama, Slovenia. *Journal of Cave and Karst Studies, 74*(3), 235–242.

Anirudhan, I. V. (2014). Significance of case studies in geotechnical engineering. In *Proceedings of Indian geotechnical conference*, December 18–20, Kakinada, India.

Bhagyalekshmi, S., Mohan, M., Sreedharan, K., & Ajaykumar, B. (2015). Evaluation of the factors controlling the spatial distribution of soil piping: A case study from the southern Western Ghats, India. *Arabian Journal of Geosciences, 8,* 8055–8067.

Cardarelli, E., Cercato, M., Cerreto, A., & Di Filippo, G. (2010). Electrical resistivity and seismic refraction tomography to detect buried cavities. *Geophysical Prospecting, 58,* 685–695.

Claerbout, J. F. (1985). *Fundamentals of geophysical data processing: With applications to petroleum prospecting*. California: Blackwell Scientific Publications.

Deco Geophysical. (2008). *RadExplorer*^{TM}. Moscow: Deco Geophysical.

Dobecki, T. L., & Upchurch, S. B. (2006). Geophysical applications to detect sinkholes and ground subsidence. *The Leading Edge, 25,* 336–341.

El-Qady, G., Hafez, M., Abdella, M. A., & Ushijima, K. (2005). Imaging subsurface cavities using geoelectric tomography and ground-penetrating radar. *Journal of Cave and Karst Studies, 67*(3), 174–181.

Ferland, J. A. (1969) Seismic mapping of cavities and voids. In *Proceedings of the twentieth annual highway geology symposium on geology as applied to highway engineering*, April 17–19 (pp. 92–98). Urbana-Champaign, IL: University of Illinois.

Gambetta, M., Armadillo, E., Carmisciano, C., Stefanelli, P., Cocchi, L., & Tontini, F. C. (2011). Determining geophysical properties of a near-surface cave through integrated microgravity vertical gradient and electrical resistivity tomography measurements. *Journal of Cave and Karst Studies, 73*(1), 11–15.

Gidigasu, M. D. (1976). *Laterite soil engineering, pedogenesis and engineering principles* (pp. 1–554). New York: Elsevier Scientific Publishing Company.

Kasthurba, A. K., Santhanam, M., & Mathews, M. S. (2007). Investigation of laterite stones for building purpose from Malabar region, Kerala State, SW India—Part 1: Field studies and profile characterization. *Construction and Building Materials, 21,* 73–82.

Kaufmann, G., Romanov, D., & Nielbock, R. (2011). Cave detection using multiple geophysical methods: Unicorn Cave, Harz Mountains, Germany. *Geophysics, 76*(3), B71–B77.

Narayanaswamy. (2004). Geological significance and significance of laterites of Kerala with special references to laterite gold occurrence in Nilambur Valley. In R. Kumar, et al. (Eds.), *Earth system science and natural resource management*, Silver Jubilee Compadium. Thiruvananthapuram: CESS.

Nolan, J. J., Miller, R., Ivanov, J., Peterie, S., & Lindgren E. (2013). Near-surface salt dissolution void identification using passive MASW. In *SEG Technical Program Expanded Abstracts* (pp. 2212–2217). https://doi.org/10.1190/segam2013-1146.1

Orfanos, C., & Apostolopoulos, G. (2012). Analysis of different geophysical methods in the detection of an underground opening at a controlled test site. *Journal of the Balkan Geophysical Society, 15,* 7–18.

Park, C. B., Miller, R. D., & Xia, J. (1999). Multichannel analysis of surface waves. *Geophysics, 64*(3), 800–808.

Prasad, T. K. (2014). PhD Thesis on geographical analysis of changing land use pattern of Kannur District in Kerala with special reference to laterite mining. Department of Geography, School of Earth and Atmospheric Sciences, Madurai Kamaraj University.

Reynolds, J. M. (1997). *An introduction to applied environmental geophysics* (p. 796). West Sussex: Wiley.

Sajinkumar, K. S., Anbazhagan, S., Pradeepkumar, A. P., & Rani, V. R. (2011). Weathering and landslide occurrences in parts of Western Ghats, Kerala. *Journal of Geological Society of India, 78*(3), 249–257.

Samsudin, H. T. (2003). A Micrograva survey over deep limestone bedrock. *Geological Society of Malaysia Bulletin, 46,* 201–208.

Sandmeier, K. J. (2009). *ReflexWTM*. Sandmeier Scientific Software: Sandmeier Scientific Software.

Twidale, C. R. (1987). Sinkholes in lateritised sediments, Western Sturt Plateau, Northern Territory, Australia. *Geomorphology, 1,* 33–52.

Tzanis, A. (2006). MATGPR: A freeware MATLAB package for the analysis of common-offset GPR data. *Geophysical Research Abstracts, 8,* 09488.

Uchida, T., & Mizuyama, T. (2002). The contribution of pipe flow on shallow landslide initiation at steep hill slopes. In *International congress: INTRAPRAEVENT 2002 in the Pacific Rim*, Matsumoto, Japan, Congress publication, 2 (pp. 559–569).

Wadia, D. N. (1945). Soils of India. *Journal of Scientific and Industrial Research, 3,* 359–367.

WTS Limited. (2013). *Geophysical investigation on 'soil piping' for Centre for Earth Science Studies (CESS)*, Trivandrum at Cherupuzha Site, Kannur District, Kerala, India. Report No: WTS/ERT/CESS/112/Rev-2.

(Received July 1, 2017, revised May 15, 2018, accepted May 24, 2018, Published online June 7, 2018)